Turbo Decoding Performance of Spectrally Efficient RS Convolutional Concatenated Codes

Li Chen
School of Information Science and Technology, Sun Yat-sen University, Guangzhou, China
Email: chenli55@mail.sysu.edu.cn

***Abstract*—Reed-Solomon convolutional concatenated (RSCC) codes have been widely used in wireless and space communications. Turbo decoding of the concatenated code has been recently developed and shown that the code's error-correction capability can be significantly improved. Particularly, turbo decoding of RSCC codes yields a competent performance when the codeword length is limited. This makes the code a very good candidate for certain communication scenarios in which short packet length is preferred and strict decoding latency and energy consumption constraints are applied, such as the wireless sensor networks (WSN) and high mobility communications (HMC). However, code concatenation inevitably results in rate loss which affects the transmission spectral efficiency. Therefore, this paper investigates the turbo decoding performance of RSCC codes that is integrated with high order modulation schemes to realize spectrally efficient transmissions. The EXtrinsic Information Transfer (EXIT) analysis of the turbo decoding mechanism is performed in order to design the inner convolutional code which can optimize the concatenated code's error-correction performance. Our simulation results obtained in both the additive white Gaussian noise (AWGN) and Rayleigh fading channels show turbo decoding of RSCC codes achieves significant performance improvements over the existing non-iterative decoding schemes.**

***Index Terms*—Concatenated codes, convolutional codes, turbo decoding, Reed-Solomon codes, spectral efficiency.**

I. Introduction

Reed-Solomon convolutional concatenated (RSCC) codes have been widely used in wireless and space communications [1] [2]. The currently used decoding scheme for the concatenated code is the one-shot Viterbi-Berlekamp-Massey (Viterbi-BM) algorithm. It is efficient in terms of running time but with limited error-correction capability. The concatenated code's performance has been later improved by various iterative attempts [3] [4] [5]. However, without an efficient approach to determine the RS coded bits' extrinsic information, they are yet to become a truly turbo decoding mechanism that iteratively exchanges the soft information between the inner and outer decoders. Consequently, the concatenated code's error-correction potential has not been well unexploited.

Until recently, a truly turbo decoding mechanism for RSCC codes was proposed in [6] [7]. In the turbo decoding scheme, the Bahl-Cocke-Jelinek-Raviv (BCJR) algorithm [8] is used to decode the inner code, providing extrinsic probabilities for the interleaved RS coded bits. They are then utilized by the outer decoding algorithm that consists of two stages. The adaptive belief propagation (ABP) algorithm [9] [10] determines the extrinsic probabilities and the *a posteriori* probabilities (APP) of RS coded bits. With the APP, decoding of an RS codeword is finalized by an algebraic algorithm, e.g., Koetter-Vardy (KV) algorithm [11] or BM algorithm [12]. After decoding all the outer codes, extrinsic probabilities of the undecoded RS bits and deterministic probabilities of the decoded RS bits will be fed back for the next iteration. Results of [6] show that such a turbo decoding mechanism achieves significant performance improvements over various existing algorithms [3] [4]. Especially when the codeword length is limited, e.g., with around a thousand bits, up to 2dB decoding gain can be achieved over the Viterbi-BM algorithm. Since the decoding complexity is proportional to codeword length, short codes have an inherited feature of low decoding complexity but with limited decoding performance. It is important to obtain a good tradeoff between the decoding performance and complexity. RSCC codes powered by turbo decoding tend to meet this demand. Although decoding of the outer codes requires both the ABP and algebraic decodings, the decoding of several RS codes can be performed in parallel, and the outer decoding latency can be reduced by a constant factor that is the depth of the block interleaver. Therefore, the concatenated code is a very competent candidate to be applied in certain communication scenarios which transmit short data packets and have a strict decoding latency constraint and limited energy consumption budget. They include the wireless sensor networks (WSN) which transmit short data packets and has a limited energy budget, and the high mobility communications (HMC) which have a strict decoding latency constraint.

However, code concatenation inevitably leads to rate loss of the system, which affects the transmission spectral efficiency. To compensate the rate loss, one solution is to puncture the output of the inner code. But it results in a significant performance loss due to the weakening of the inner code's error-correction capability [6]. The alternative solution is to integrate the RSCC code with a high order modulation scheme. Hence, this paper investigates the turbo decoding performance of spectrally efficient RSCC codes that are integrated with high order modulation schemes. We aim to reveal RSCC codes' performance potential under such scenarios. The EXtrinsic Information Transfer (EXIT) [13] characteristics of the decoding is investigated, which provides the insight in designing the inner codes. Turbo decoding performance of the spectrally efficient RSCC codes is further evaluated in both the additive white Gaussian noise (AWGN) and Rayleigh fading channels and its suitability to be applied in WSN and HMC will also be demonstrated.

II. RSCC Codes

Let $\mathbb{F}_q = \{0, 1, \alpha, \ldots, \alpha^{q-2}\}$ denote the finite filed of size q, where α is the primitive element of the field. In this paper, it is assumed that $q = 2^\omega$ and ω is a positive integer. The message vector of an (n, k) RS code can be written as

$$\overline{U} = [U_1\ U_2\ \ldots\ U_k] \in \mathbb{F}_q^k, \tag{1}$$

where n and k are the length and dimension of the code, respectively, and $n = q-1$. The outer code rate is $r_{\text{out}} = k/n$. The generator matrix of the RS code is defined as

$$\mathbf{G} = \begin{pmatrix} 1 & 1 & \cdots & 1 \\ 1 & \alpha & \ldots & \alpha^{n-1} \\ \vdots & \vdots & \ddots & \vdots \\ 1 & \alpha^{k-1} & \ldots & \alpha^{(k-1)(n-1)} \end{pmatrix}, \tag{2}$$

and the RS codeword can be generated by

$$\overline{C} = \overline{U} \cdot \mathbf{G} = [C_1\ C_2\ \ldots\ C_n] \in \mathbb{F}_q^n. \tag{3}$$

To perform the ABP decoding, the RS code's parity-check matrix is needed. For an (n, k) RS code, it is defined as

$$\mathbf{H} = \begin{pmatrix} 1 & \alpha & \cdots & \alpha^{n-1} \\ 1 & \alpha^2 & \ldots & \alpha^{2(n-1)} \\ \vdots & \vdots & \ddots & \vdots \\ 1 & \alpha^{n-k} & \ldots & \alpha^{(n-k)(n-1)} \end{pmatrix}. \tag{4}$$

Let $\mathbf{A}$ denote the companion matrix of a primitive polynomial of $\mathbb{F}_q$ and it is a $\omega \times \omega$ binary matrix. The binary image of $\mathbf{H}$ can be generated by mapping its entries $\alpha^i \mapsto \mathbf{A}^i$ and $i = 0, 1, \ldots, q-2$, resulting in the binary parity-check matrix $\mathbf{H}_b$ with size $(n-k)\omega \times n\omega$.

If the depth of the block interleaver is D, D RS codewords will be generated by (3) and then interleaved. Following the conventions, D is set as ten throughout the paper. The interleaved RS codeword symbols are converted into an RS coded bit sequence $c_1, c_2, \ldots, c_{Dn\omega}$, which is the input to the convolutional encoder whose transfer functions are denoted in the octal form. If the inner code rate is r_{in}, the inner encoder yields a convolutional coded bit sequence of $v_1, v_2, \ldots, v_{Dn\omega/r_{\text{in}}}$. They will be modulated for transmission.

Based on the above description, the rate of the concatenated code is $r = r_{\text{out}} r_{\text{in}}$. Code concatenation will inevitably lead to rate loss and it affects the spectral efficiency of an RSCC coded communication system. If the order of the modulation scheme is m bits/sym, the spectral efficiency of an RSCC coded system is

$$\xi = r_{\text{out}} r_{\text{in}} m \text{ bits/sym}. \tag{5}$$

Therefore, one approach to maintain a high spectral efficiency is to puncture the output of the inner encoder. However, it has been shown that such an approach leads to a significant performance loss [6]. The alternative approach is to utilize a high order modulation scheme, while leaving the error-correction capability of the inner code intact. This paper will investigate the latter approach in realizing spectrally efficient transmission of RSCC codes.

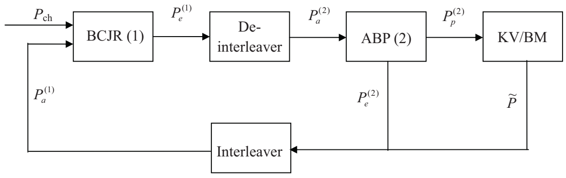

Fig. 1. Turbo decoding block diagram.

III. Turbo Decoding

The turbo decoding block diagram is shown as Fig.1. Decoding of the inner and outer codes are performed by the BCJR algorithm [8] and the ABP-KV(BM) algorithm [9] [10], respectively. P_a, P_e and P_p are used to denote the *a priori*, extrinsic and *a posteriori* probabilities, respectively. Their superscripts of (1) and (2) indicate the probability is associated with the BCJR algorithm and the ABP algorithm, respectively.

A. BCJR Decoding of the Inner Code

In this paper, it is assumed that $r_{\text{in}} = \frac{1}{2}$ and hence BCJR decoding of the inner code will be described in light of a rate half convolutional code. Given $\overline{\mathcal{Y}} \in \mathbb{R}$ as the received vector, we can obtain the channel observations $P_{\text{ch}}[v_i = \theta|\overline{\mathcal{Y}}]$ that indicates the conditional probability of bit v_i being θ, where $i = 1, 2, \ldots, 2Dn\omega$ and $\theta \in \{0, 1\}$. In the code's trellis, if an input of $c_i = \theta$ yields two coded bits of $(v_{2i-1}, v_{2i}) = (\theta_1, \theta_2)$ where $i = 1, 2, \ldots, Dn\omega$ and $(\theta_1, \theta_2) \in \{0, 1\}$, and it triggers a trellis state transition whose probability is determined by

$$\Gamma_i = P_a^{(1)}[c_i = \theta] P_{\text{ch}}[v_{2i-1} = \theta_1|\overline{\mathcal{Y}}] P_{\text{ch}}[v_{2i} = \theta_2|\overline{\mathcal{Y}}]. \tag{6}$$

In the beginning, no knowledge of the interleaved RS coded bits is available and $P_a^{(1)}[c_i = \theta]$ will be initialized as $P_a^{(1)}[c_i = 0] = P_a^{(1)}[c_i = 1] = \frac{1}{2}$. In the following iterations, $P_a^{(1)}[c_i = \theta]$ will be updated by the feedbacks of the outer decoding. With the trellis state transition probabilities, the forward and backward traces will be performed to determine the APP of the interleaved RS coded bits, i.e., $P_p^{(1)}[c_i = \theta|\overline{\mathcal{Y}}]$. Their extrinsic probabilities are determined by

$$P_e^{(1)}[c_i = \theta] = \mathcal{N}_e \frac{P_p^{(1)}[c_i = \theta|\overline{\mathcal{Y}}]}{P_a^{(1)}[c_i = \theta]}, \tag{7}$$

where $\mathcal{N}_e = \sum_{\theta \in \{0,1\}} P_e^{(1)}[c_i = \theta]$ is a normalization factor.

Probabilities $P_e^{(1)}$ are then deinterleaved during which every ω consecutive pairs of extrinsic probabilities are grouped to represent an RS codeword symbol. The deinterleaved extrinsic probabilities will be utilized by the following outer decoding.

B. ABP-KV(BM) Decoding of the Outer Code

By reading out each row of the deinterleaver and performing the following mapping

$$P_e^{(1)}[c_i = \theta] \mapsto P_a^{(2)}[c_i = \theta], \tag{8}$$

we can obtain the *a priori* probability for each bit of an RS codeword and $i = 1, 2, \dots, n\omega$. The *a priori* log-likelihood ratio (LLR) value of bit c_i is determined by

$$L_{a,i} = \ln\Big(\frac{P_a^{(2)}[c_i = 0]}{P_a^{(2)}[c_i = 1]}\Big). \tag{9}$$

And the *a priori* LLR vector of an RS codeword is

$$\overline{L}_a = [L_{a,1}\ L_{a,2}\ \dots\ L_{a,(n-k)\omega}\ \dots\ L_{a,n\omega}]. \tag{10}$$

Notice that an LLR value with a higher magnitude of $|L_{a,i}|$ implies the bit is more reliable. The ABP algorithm will first sort vector $\overline{L}_a$ according to each bit's magnitude, aiming to identify the $(n-k)\omega$ least reliable bits. Their corresponding columns in $\mathbf{H}_b$ will be reduced to weight-1 columns by Gaussian elimination. The sorting yields a refreshed bit index sequence $\delta_1, \delta_2, \dots, \delta_{(n-k)\omega}, \dots, \delta_{n\omega}$ which implies $|L_{a,\delta_1}| < |L_{a,\delta_2}| < \cdots < |L_{a,\delta_{(n-k)\omega}}| < \cdots < |L_{a,\delta_{n\omega}}|$. We now know $c_{\delta_1}, c_{\delta_2}, \dots, c_{\delta_{(n-k)\omega}}$ are the $(n-k)\omega$ least reliable bits. Let Υ_δ denote a weight-1 column with 1 at its δth entry. With the sorting outcome, Gaussian elimination will reduce column δ_1 to Υ_1, then reduce column δ_2 to Υ_2, and etc. It delivers an adapted parity-check matrix $\mathbf{H}'_b$ that has an $(n-k)\omega \times (n-k)\omega$ identity submatrix.

Let $h_{ji} \in \{0, 1\}$ denote the entry of $\mathbf{H}'_b$ and we define

$$\mathbf{J}(i) = \{j \mid h_{ji} = 1,\ \forall\ 1 \le j \le (n-k)\omega\}, \tag{11}$$

$$\mathbf{I}(j) = \{i \mid h_{ji} = 1,\ \forall\ 1 \le i \le n\omega\}. \tag{12}$$

The iterative BP process is performed based on the Tanner graph that is defined by $\mathbf{H}'_b$. The extrinsic LLR value for each RS coded bit can be determined by

$$L_{e,i} = \sum_{j \in \mathbf{J}(i)} 2\tanh^{-1}\Big(\prod_{\tau \in \mathbf{I}(j)\setminus i} \tanh\Big(\frac{L_{a,\tau}}{2}\Big)\Big). \tag{13}$$

After a moderate number of BP iterations, the *a posteriori* LLR of each RS coded bit is determined by

$$L_{p,i} = L_{a,i} + \eta L_{e,i}, \tag{14}$$

where $\eta \in (0, 1]$ is the damping factor [9]. Consequently, the *a posteriori* LLR vector of an RS codeword is

$$\overline{L}_p = [L_{p,1}\ L_{p,2}\ \dots\ L_{p,(n-k)\omega}\ \dots\ L_{p,n\omega}]. \tag{15}$$

If there are multiple Gaussian eliminations, the *a posteriori* LLR vector will be fed back and mapped to $\overline{L}_a$ as

$$\overline{L}_p \mapsto \overline{L}_a. \tag{16}$$

Based on the updated $\overline{L}_a$ vector, the next round bit reliability sorting and Gaussian elimination will be performed. With each adapted matrix $\mathbf{H}'_b$, a number of BP iterations will be carried out, delivering both the extrinsic and the *a posteriori* LLR values. Consequently, extrinsic probabilities and APP of RS coded bits are

$$P_e^{(2)}[c_i = 0] = \frac{1}{1 + e^{-L_{e,i}}},\ P_e^{(2)}[c_i = 1] = \frac{1}{1 + e^{L_{e,i}}}, \tag{17}$$

and

$$P_p^{(2)}[c_i = 0] = \frac{1}{1 + e^{-L_{p,i}}},\ P_p^{(2)}[c_i = 1] = \frac{1}{1 + e^{L_{p,i}}}. \tag{18}$$

With each adapted parity-check matrix $\mathbf{H}'_b$, we can obtain all the bit extrinsic probabilities and APP of an RS codeword. The APP will be utilized by an algebraic algorithm that finalizes the decoding of an RS codeword. Specifically, if KV decoding [11] is utilized, a symbol wise reliability matrix $\mathbf{\Pi}$ of size $q \times n$ will be formed with which the algebraic list decoding process will be performed to find the decoding output candidates. If BM decoding [12] is utilized, a hard-decision received word $\overline{R}$ will be formed with which the syndrome based unique decoding process will be performed. It is well known that KV decoding has a greater error-correction capability, but at the cost of higher decoding complexity. In turbo decoding of RSCC codes, the second stage outer decoding plays a less important role in determining the error-correction performance. Hence, when the decoding efficiency is a critical issue for a system, BM algorithm should be employed.

With multiple Gaussian eliminations, multiple algebraic decodings will be performed. This may result in giving plural decoding output candidates, among which the maximal likelihood (ML) criterion [14] will be utilized to identify the most likely codeword. If it has been found, the current outer decoding will be terminated and we can obtain the deterministic probabilities of the corresponding RS coded bits. In particular, if the algebraic decoding estimates bit $c_i = 0$, then its deterministic probability is $\tilde{P}[c_i = 0] = 1$ and $\tilde{P}[c_i = 1] = 0$. Otherwise, $\tilde{P}[c_i = 0] = 0$ and $\tilde{P}[c_i = 1] = 1$. Therefore, after decoding all the D RS codewords, extrinsic probabilities $P_e^{(2)}$ of the undecoded bits and deterministic probabilities $\tilde{P}$ of the decoded RS bits will be fed back. They are interleaved and mapped to $P_a^{(1)}$ as

$$P_e^{(2)}[c_i = \theta],\ \tilde{P}[c_i = \theta] \mapsto P_a^{(1)}[c_i = \theta]. \tag{19}$$

The decoded RS codeword will not be processed again in the coming iterations. Therefore, turbo decoding of the concatenated code is performed in a successive cancellation manner such that the decoding is completed either when all the D RS codewords have been decoded or the designed maximal turbo iteration number is reached.

IV. Design of the Inner Code

The EXIT analysis of the turbo decoding algorithm is presented, aiming to shed lights on design of the inner convolutional code. So that, turbo decoding performance of the concatenated codes can be optimized. Specifically, by analyzing the interplay between the EXIT curve of the BCJR algorithm and the inverted EXIT curve of the ABP-

KV algorithm [1], we try to identify the signal-to-noise ratio (SNR) value at which an exit tunnel starts to exist. Such a SNR value is called the decoding pinch-off SNR limit and denoted as $\mathrm{SNR}_{\mathrm{off}}$. Since the existence of an exit tunnel implies the iterative decoding mechanism is functioning with a tendency of providing a valid codeword, the $\mathrm{SNR}_{\mathrm{off}}$ indicates the position at which waterfall of the turbo decoder's bit error rate (BER) curve starts to happen [13]. Therefore, the inner code should be chosen such that it yields a lower $\mathrm{SNR}_{\mathrm{off}}$ value. With such an inner code, turbo decoding of the concatenated code will show a better iterative decoding convergence which leads to a better BER performance. Moreover, since turbo decoding of the concatenated code is performed in a successive cancellation manner, when the SNR is sufficiently high, most of the decoding events can decode all the RS codewords in the first round. Hence, the inner code's free distance is also an important factor in determining the code's asymptotic performance. Our design will look into both of these two factors. Since the author's earlier work [6] showed the systematic feedback convolutional codes yield a better performance than their nonsystematic counterparts, our design will fucus on the systematic feedback ones.

Let $\mathcal{I}_a^{(1)}$ and $\mathcal{I}_e^{(1)}$ denote the mutual information of the *a priori* probabilities and that of the extrinsic probabilities of the BCJR algorithm, respectively. Similarly, $\mathcal{I}_a^{(2)}$ and $\mathcal{I}_e^{(2)}$ are utilized to denote the mutual information that are associated with the ABP-KV algorithm. In determining the mutual information $\mathcal{I}_e^{(2)}$, the feedback probabilities of all the D RS codewords are taken into account, i.e.,

$$\mathcal{I}_e^{(2)} = 1 - \frac{1}{Dn\omega} \sum_{i=1}^{Dn\omega} \mathcal{H}_b(P^{(2)}[c_i = \theta]), \tag{20}$$

where $P^{(2)}[c_i = \theta] = \tilde{P}[c_i = \theta]$ if bit c_i is decoded, or $P^{(2)}[c_i = \theta] = P_e^{(2)}[c_i = \theta]$ otherwise. $\mathcal{H}_b(\cdot)$ is the binary entropy function.

Moreover, the ABP process is performing with two Gaussian eliminations and for each adapted parity-check matrix, there are two BP iterations. KV process is performing with a designed factorization output list size of ten. Those ABP-KV decoding parameters will be adopted in the simulations of Section V. Let $\mathcal{T}^{(1)}$ denote the extrinsic-*a priori* transfer function of the BCJR algorithm which decodes the inner code, the EXIT curve of the BCJR algorithm shows

$$\mathcal{I}_e^{(1)} = \mathcal{T}^{(1)}(\mathcal{I}_a^{(1)}, \mathrm{SNR}). \tag{21}$$

Similarly, if $\mathcal{T}^{(2)}$ denotes the extrinsic-*a priori* transfer function of the ABP-KV algorithm, the EXIT curve of the ABP-KV algorithm shows

$$\mathcal{I}_e^{(2)} = \mathcal{T}^{(2)}(\mathcal{I}_a^{(2)}). \tag{22}$$

Fig.2 shows the EXIT performance of turbo decoding a concatenated code in which the outer code is the RS

[1] In the EXIT analysis, the ABP-KV algorithm is chosen as the outer decoding algorithm.

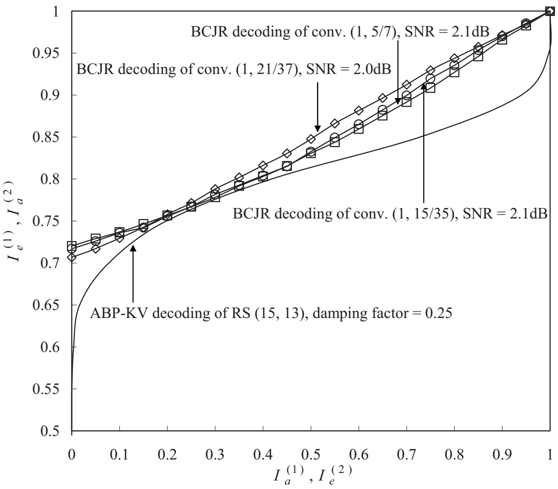

Fig. 2. EXIT performance of the RS (15, 13)-conv. concatenated codes. Gray labelling 16QAM is utilized for transmission over the AWGN channel.

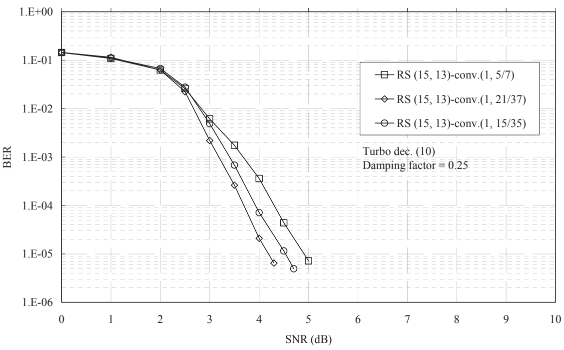

Fig. 3. Turbo decoding performance of the RS (15, 13)-conv. concatenated codes with Gray labelling 16QAM over the AWGN channel.

(15, 13) code. The inner code candidates include the conv.$(1, 5/7)_8$ code, the conv.$(1, 21/37)_8$ code and the conv.$(1, 15/35)_8$ code. The first code has four states and the other two codes have 16 states. The Gray labelling 16QAM is utilized realizing a transmission spectral efficiency of $\xi = 1.73$ bits/sym over the AWGN channel. Among the three candidates, the conv.$(1, 21/37)_8$ yields the lowest $\mathrm{SNR}_{\mathrm{off}}$ value and its 16-state trellis architecture ensures it a larger free distance than the conv.$(1, 5/7)_8$ code. Hence, the RS (15, 13)-conv.$(1, 21/37)_8$ code should outperform the RS (15, 13)-conv.$(1, 5/7)_8$ and the RS (15, 13)-conv.$(1, 15/35)_8$ codes. In comparison of the RS (15, 13)-conv.$(1, 5/7)_8$ code and the RS (15, 13)-conv.$(1, 15/35)_8$ code, the latter one should prevail, since its inner code has a larger free distance despite both of the inner codes yield the same $\mathrm{SNR}_{\mathrm{off}}$ value. Fig.3 validates the EXIT prediction by showing the BER performance of turbo decoding the three concatenated codes. The number of turbo decoding iterations is ten. It shows that the RS (15, 13)-conv.$(1, 21/37)_8$ code outperforms the other two.

Fig.4 shows the EXIT performance of turbo decoding

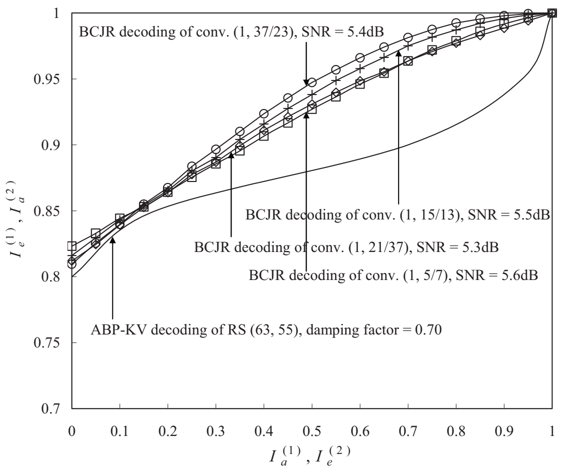

Fig. 4. EXIT performance of the RS (63, 55)-conv. concatenated codes. Gray labelling 64QAM is utilized for transmission over the AWGN channel.

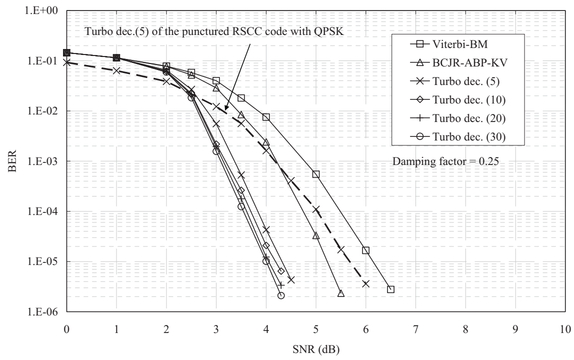

Fig. 5. Turbo decoding performance of the RS (15, 13)-conv.$(1, 21/37)_8$ code with Gray labelling 16QAM over the AWGN channel.

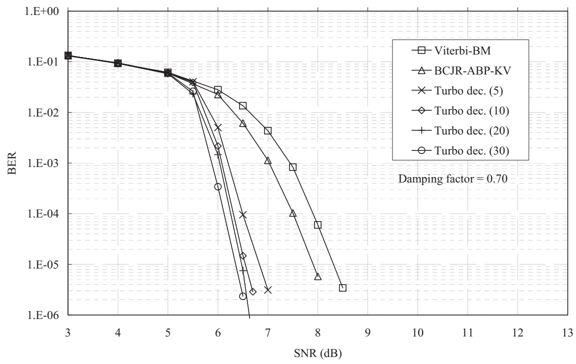

Fig. 6. Turbo decoding performance of the RS (63, 55)-conv.$(1, 21/37)_8$ code with Gray labelling 64QAM over the AWGN channel.

a concatenated code in which the outer code is the RS (63, 55) code. The inner code candidates include the conv.$(1, 5/7)_8$ code, the conv.$(1, 15/13)_8$ code, the conv.$(1, 21/37)_8$ code and the conv.$(1, 37/23)_8$ code. They have 4, 8, 16 and 16 states, respectively. Gray labelling 64QAM modulation is employed, realizing a transmission spectral efficiency of $\xi = 2.62$ bits/sym over the AWGN channel. Following a similar argument, the conv.$(1, 21/37)_8$ code should again be chosen as an inner code in the concatenated scheme. Simulation results of turbo decoding of the above EXIT designed RSCC codes will be presented in the following section.

V. Simulation Results

This section presents the above designed spectrally efficient RSCC codes over both the AWGN and Rayleigh fading channels. Although the EXIT design of Section IV was conducted in the AWGN channel, we will inherit the designed code to evaluate its performance over the Rayleigh fading channel. Our comparison benchmark schemes include the currently used Viterbi-BM algorithm and the BCJR-ABP-KV(BM) algorithm [15] both of which are one-shot decoding algorithms. In the following discussions, decoding gains are quantized at the BER of 10^{-5}. Without specifically mentioning, KV algorithm is utilized in the turbo decoding process.

Fig.5 shows the BER performance of the RS (15, 13)-conv.$(1, 21/37)_8$ code which is integrated with Gray labelling 16QAM. It can be seen that turbo decoding achieves significant performance improvements over the benchmark algorithms. E.g., performing turbo decoding with five iterations yields 1.9dB gain over the Viterbi-BM algorithm. By increasing the iteration budget to 30, it yields an extra 0.3dB gain. In order to demonstrate the advantage of using a high order modulation scheme rather than puncturing the output of the inner code, Fig.5 further reveals the turbo decoding performance of the same concatenated code that is punctured. The puncture rate is 1/2 [2] and Gray labelling QPSK is utilized, resulting in the same spectral efficiency of 1.73 bits/sym. It can be seen that puncturing the output of the inner code leads to a sizable performance loss. This is because puncturing results in a rate 1 inner code whose error-correction capability is deprived. Note that the RS (15, 13)-conv.$(1, 21/37)_8$ code has a moderate codeword length of 1200 bits. Such a data packet size is preferred in WSN. Its powerful error-correction performance makes it a competent code for WSN. Furthermore, Fig.6 shows the BER performance of the RS (63, 55)-conv.$(1, 21/37)_8$ code with Gray labelling 64QAM. It again shows that significant performance improvements can be obtained. Performing turbo decoding with 30 iterations achieves 1.9dB gain over the Viterbi-BM algorithm.

Turbo decoding performance of the RS (63, 55)-conv.$(1, 21/37)_8$ code with Gray labelling 64QAM over the Rayleigh fading channels is shown by Fig.7. The Rayleigh fading channel profile is generated by Jakes' method [16] through setting the mobile user's velocity and the signal carrier frequency. The carrier frequency is set as 1.9 GHz which is in line with most of the 3G standards. While the velocity is set as 350 km/hr and 200 km/hr,

[2]The parity bits are punctured out.

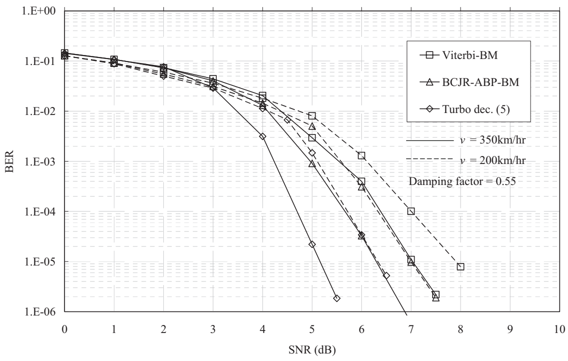

Fig. 7. Turbo decoding performance of the RS (63, 55)-conv.$(1, 21/37)_8$ code with Gray labelling 64QAM over Rayleigh fading channels.

with which the author aims to investigate the concatenated code's performance in HMC. E.g., the 350 km/hr setup represents the communication with a mobile user in a high speed train, and the 200 km/hr setup represents the vehicle-to-vehicle (V2V) communication scenario. In both of the cases, it is assumed that every 30 64QAM symbols experience a channel fading realization. In order to better capture the block fading diversity, transmission of the concatenated code is assisted by the bit-interleaved coded modulation (BICM). That implies the output of inner code will be converted into six parallel bit streams. Each bit stream will be randomly interleaved and every six bits from the six interleaved streams will be mapped to a 64QAM symbol for transmission. Before the decoding, a corresponding signal detection process will be performed with the knowledge of channel state information. Considering the strict decoding latency constraint for HMC, the second stage outer decoding is performed by BM algorithm. Since the decoding of D RS codewords can be performed in parallel and the decoding latency can be reduced by a constant factor of D, leveraging it to that of decoding a single RS (63, 55) code. Fig.7 shows that the turbo decoding algorithm yields significant decoding gains over the benchmark schemes. Overall, powered by both BICM and the turbo decoding mechanism, RSCC codes can also be applied in HMC scenarios.

VI. Conclusion

This paper has investigated turbo decoding performance of the spectrally efficient RSCC codes that are integrated with a high order modulation scheme, e.g., 16QAM or 64QAM. Powered by the turbo decoding mechanism, RSCC codes yield a competent performance with moderate codeword length, e.g, with about a thousand bits. This makes the concatenated code a very good candidate to be applied in WSN in which data packet size is limited. Moreover, since short code has an inherited feature of low decoding latency which is a critical issue for HMC, RSCC codes are also very good candidates to be applied in such scenarios. The EXIT analysis has been conducted in designing a suitable inner code for optimizing the turbo decoding performance. Our simulation results have demonstrated that with maintaining a high spectral efficiency, the turbo decoding algorithm achieves significant performance improvements over the conventional one-shot decoding algorithms.

Acknowledgement

This research is supported by the National Basic Research Program of China (973 Program) with project ID 2012CB316100 and the National Natural Science Foundation of China (NSFC) with project ID 61372079.

References

[1] R. Cideciyan, E. Eleftheriou and M. Rupf, "Concatenated Reed-Solomon/convolutional coding for data transmission in CDMA-based cellular systems," *IEEE Trans. Commun.*, vol. 45 (10), pp. 1291-1303, Oct. 1997.

[2] Consultative Committee for Space Data Systems, "Recommendation for space data systems standard, telemetry channel coding," CCSDS 101.0-B-6, *Blue Book*, issue 6, Oct. 2002.

[3] E. Paaske, "Improved decoding for a concatenated coding system recommended by CCSDS," *IEEE Trans. Commun.*, vol. 38 (8), pp. 1138-1144, Aug. 1990.

[4] J. Zhang, J. You, L. Lu and X. Ma, "An iterative soft-decision decoding algorithm for conventional concatenated codes," in *Proc. the 4th Int. Conf. Commun. and Netw. in China*, Xi'an, China, Aug. 2009.

[5] M. Lamarca, J. Sala and A. Martinez, "Iterative decoding algorithms for RS-convolutional concatenated codes," *Proc. the 3rd Int. Symp. Turbo Codes*, Brest, France, Sept. 2005.

[6] L. Chen, "Iterative soft decoding of Reed-Solomon convolutional concatenated codes," *IEEE Trans. Commun.*, to appear.

[7] L. Chen and X. Ma, "Iterative soft-decision decoding of Reed-Solomon convolutional concatenated codes," *Proc. the IEEE Int. Symp. Inform. Theory (ISIT)*, Istanbul, Turkey, Jul. 2013.

[8] L. R. Bahl, J. Cocke, F. Jelinek and J. Raviv, "Optimal decoding of linear codes for minimizing symbol error rate," *IEEE Trans. Inform. Theory*, vol.20 (2), pp. 284-287, Mar. 1974.

[9] M. El-Khamy and R. McEliece, "Iterative algebraic soft-decision list decoding of Reed-Solomon codes," *IEEE J. Sel. Area in Commun.*, vol.24 (3), pp. 481-490, Mar. 2006.

[10] J. Jiang and K. Narayanan, "Iterative soft-input-soft-output decoding of Reed-Solomon codes by adapting the parity check matrix," *IEEE Trans. Inform. Theory*, vol. 52 (8), pp. 3746-3756, Aug. 2006.

[11] R. Koetter and A. Vardy, "Algebraic soft-decision decoding of Reed-Solomon codes," *IEEE Trans. Inform. Theory*, vol. 49 (11), pp. 2809-2825, Nov. 2003.

[12] J. L. Massey, "Shift register synthesis and BCH decoding," *IEEE Trans. Inform. Theory*, vol. 15, pp. 122-127, 1969.

[13] S. ten Brink, "Convergence behavior of iteratively decoded parallel concatenated codes," *IEEE Trans. Commun.*, vol. 49 (10), pp. 1727-1737, Oct. 2001.

[14] T. Kaneko, T. Nishijima, H. Inazumi and S. Hirasawa, "An efficient maximum-likelihood-decoding algorithm for linear block codes with algebraic decoder," *IEEE Trans. Inform. Theory*, vol. 40 (2), pp. 320-327, Mar. 1994.

[15] L. Chen, "Improved soft-decision decoding of RSCC codes," *Proc. the IEEE Wirel. Commun. Netw. Conf. (WCNC)*, Shanghai, China, Apr. 2013.

[16] W. Jakes. Ed., *Microwave Mobile Communications,* New Jersey, IEEE Press, 1993.